

## DEEP *EINSTEIN* X-RAY IMAGERY OF THE SMALL MAGELLANIC CLOUD

FREDERICK C. BRUHWEILER<sup>1</sup>

Department of Physics, Catholic University of America

AND

DANIEL A. KLINGLESMTIH III,<sup>2</sup> THEODORE R. GULL,<sup>1,2</sup> AND SABATINO SOFIA<sup>1,3</sup>

NASA/Goddard Space Flight Center

Received 1985 June 18; accepted 1986 November 11

### ABSTRACT

Deep *Einstein* IPC imagery of  $\sim 50\%$  of the main body and “wing” of the Small Magellanic Cloud has been obtained and analyzed. The four X-ray images have exposure times between 12,000 and 24,000 s and reveal a total of 25 X-ray sources. Twelve of these sources are new detections. Two, possibly three, sources with soft spectra may be newly discovered supernova remnants. The rest of the sources have harder spectra and intrinsic X-ray luminosities in the range  $34.0 \lesssim \log L_x \lesssim 35.0$  and are most likely stellar objects in the SMC. These luminosities are much lower than that found for typical galactic X-ray binaries, and a factor of 100 larger than the range for “normal” galactic O and B stars. The luminosities of these sources closely resemble those for galactic X-ray Be stars, but the SMC sources lack the X-ray variability that is typical for galactic Be stars. Preliminary theoretical calculations indicate that the X-ray luminosities of “normal” O and B stars should be extremely sensitive to chemical composition. If so, we cannot rule out the possibility that at least some fraction of the SMC hard X-ray sources are associated with high luminosity, “normal” O and B stars in that metal deficient galaxy. Some X-ray emission does appear to be correlated with extremely luminous OB stars, embedded in “ $\eta$  Carina-like” regions. But it is unclear if this emission is due to the individual luminous stars or the complexity of the regions in which they are embedded. Also, the positional coincidences between stars in the list of Azzopardi and Vigneau and the X-ray source positions are significant and suggest that at least some of the objects responsible for the X-ray emission represent a young population.

*Subject headings:* galaxies: Magellanic Clouds — nebulae: supernova remnants — stars: early-type — X-rays: sources

### I. INTRODUCTION

Prior to studies utilizing the *Einstein Observatory*, both the Large and Small Magellanic Clouds have been studied at X-ray wavelengths from rockets and the *Uhuru* and *SAS 3* satellites (Price *et al.* 1971; Leung *et al.* 1971; Clark *et al.* 1978). The SMC was first observed in X-rays by Price *et al.* (1971) from a rocket payload. This, and further investigations of the SMC using *Uhuru*, revealed one luminous, highly variable X-ray source, SMC X-1 (Leung *et al.* 1971). This source is the most luminous binary X-ray source known. Two additional luminous, but transient, X-ray sources, SMC X-2 and SMC X-3, have since been detected (Clark *et al.* 1978). All three of these sources have maximum X-ray luminosities in excess of  $10^{38}$  ergs  $s^{-1}$ , analogous to or exceeding the luminous X-ray binaries in our Galaxy. However, an additional somewhat weaker source, 4U 0026–73, has been also identified (Forman *et al.* 1978).

Fairly extensive X-ray surveys of both the LMC and SMC and their environs using the image proportional counter (IPC) aboard the *Einstein Observatory* (*HEAO 2*) have been published (Long, Helfand, and Grabelsky 1981; Seward and Mitchell 1981, hereafter SM). The *Einstein* survey of the LMC (Long *et al.*) detected 97 sources with luminosities ranging from  $1 \times 10^{35}$  to  $2 \times 10^{38}$  ergs  $s^{-1}$  over the energy band 0.15–4.5 keV. The SM survey covered a region exceeding 40 deg<sup>2</sup>

centered on the SMC. The exposures of their survey, typically 1000–2000 s, were comparable to those acquired of the LMC by Long *et al.* and provided rather complete coverage down to X-ray luminosities of  $L_x = 10^{36}$  ergs  $s^{-1}$ , with the faintest source detected being  $3 \times 10^{35}$  ergs  $s^{-1}$ . A total of 26 sources were considered as definite detections. Of these, five were identified with objects not associated with the SMC. Only six sources, five of which may be SNRs, appear associated with the SMC. In agreement with previous results, the most luminous of these sources was SMC X-1, while the second brightest was a previously unidentified supernova remnant (SNR) (see also § IV). Most of the X-ray sources detected in the SM (1981) survey have remained unidentified with counterparts at other wavelengths, and lie far from the main body of the SMC.

As a follow up to the initial survey of the SMC by SM, two additional groups obtained deep IPC imagery (exposures in excess of 10,000 s) which covered the entire main body as well as the so-called “wing” of the SMC. In this paper we present results based upon deep IPC imagery covering  $\sim 50\%$  of the SMC as defined by the observed stellar populations. Preliminary results for the complementary deep X-ray imagery covering the remainder of the main body of the SMC have appeared elsewhere (Inoue, Koyama, and Tanaka 1983; hereafter IKT).

### II. OBSERVATIONS

The instrumentation aboard the *Einstein Observatory* including the IPC has been previously described (Giacconi *et al.* 1979). While in operation, the IPC was sensitive to X-rays in the energy range 0.15–4.5 keV and provided some small degree

<sup>1</sup> Guest Observer with the *Einstein Observatory*.

<sup>2</sup> Also Laboratory for Astronomy and Solar Physics/GSFC.

<sup>3</sup> Also Laboratory for Atmospheres/GSFC.

of spectral resolution which can be used to determine the spectral characteristics or source hardness of the detected X-ray sources. This will be important in discriminating between the soft spectra of supernova remnants and the harder spectra of, presumably, stellar sources. The full field sampled by the IPC detector was a square region  $75' \times 75'$ . However, the edges of the field were affected by a high charged particle background. Also, vignetting produced roughly a factor of 2 "falloff" in effective sensitivity as one goes from the center of the field to the edge. Thus, the usable region was a  $60' \times 60'$  square, except for shadowing produced by narrow supporting rib structures which frame a central  $45' \times 45'$  square region.

The selection of our field centers for the deep IPC imagery was based initially upon a desire to detect faint supernova remnants in the SMC. Thus, our pointings were biased toward regions with pronounced nebular emission, especially in [O III]  $\lambda 5007$  and [S II]  $\lambda\lambda 6716, 6731$ . As a result, we used the optical H $\alpha$  emission-line survey of Davies, Elliot, and Meaburn (1976) and unpublished narrow-band optical H I, [S II], and [O III] emission-line data of one of the authors (T. R. G.) in choosing the field centers. In addition, to insure that deep imagery was obtained for the entire SMC, we minimized the overlap among the selected IPC fields of our study and that of IKT.

In Table 1, we present the relevant data for the four IPC images discussed in this work. For each IPC image, the sequence number, the field center in epoch (1950) coordinates, the total processed exposure time in seconds, and the start and end dates to the nearest minute are given.

All four IPC images have undergone data processing at the Harvard-Smithsonian Astrophysical Observatory using both old and new standard *Einstein* data reduction software as described in the *Einstein Observatory* manual (1980) and in Harnden *et al.* (1984). Data reduction performed by the old standard software, shortly after the observations were obtained, used a rather approximate representation for the background, and often yielded rather inaccurate estimates for the derived X-ray fluxes and hardness ratios. The reprocessing of our IPC data using new software was concluded near the end of 1983, and included the use of the "local detect" algorithm (a moving cell technique) which provided a much better estimate of the local background in the image pixels around the detected X-ray sources.

In Table 2, we present the X-ray sources detected in the IPC images listed in Table 1. In Figure 1, we indicate how the detected sources (Table 2) lie with respect to the body and wing of the SMC. Given in Table 2 are the source number (col. [1]), the source position in right ascension and declination for epoch 1950.0 (cols. [2], [3]), the IPC image sequence number in which the source is seen (col. [4]), the standard *Einstein*

count rate determined from IPC data (col. [5]), the associated count rate error (col. [6]), and the 90% confidence error radius in arc seconds (col. [7]). Intrinsic luminosity estimates and quantitative hardness ratios are only given for sources flagged with the new software. Many sources flagged only by the old software are identified as being either soft (S) or hard (H) sources. These qualitative hardness estimates are based upon analysis of the pulse height data in the initial data processing and examination of the computer imagery of the different energy bands. The relevant information from the  $\chi^2$  tests for source variability is contained in columns (10) and (11). Column (10) contains the associated probability, while column (11) gives the interval length in seconds and the number of intervals used in the analysis. The variability analysis is discussed more fully below. Finally, column (12) contains an estimate of the quality of the X-ray detection.

The intrinsic luminosity estimates given in Table 2, like those of SM and also IKT, assume that 1 IPC count  $s^{-1}$  corresponds to an intrinsic *Einstein* X-ray luminosity of  $2.0 \times 10^{37}$  ergs  $s^{-1}$  at the distance of the SMC (70 kpc). This estimate does not take into account the spectral characteristics of the individual sources (see § III). Because of uncertainties or differences in the shapes of the individual X-ray spectra, this estimate is accurate to within a factor of 1.5 (Seward and Mitchell 1981). Using this estimate as a guide we conclude that our source sample is complete for all point sources with  $L_x > 10^{35}$  ergs  $s^{-1}$  within the area sampled by the X-ray images discussed here. This, naturally, excludes the small areas which are effected by shadowing from the support ribs in the IPC.

One can obtain some information about intrinsic source variability from timing information. A standard  $\chi^2$  test for secular variability is routinely performed for detected sources as part of the *Einstein* guest investigation package (see Harnden *et al.*, and references therein). Since the observed count rates for the X-ray sources in the SMC are low, in order for the analysis to have significance the "clean" data, uncontaminated by high background and other effects, are binned into long equal time intervals, typically 10–16 minutes in length with 8 to 16 bins (see cols. [10] and [11] in Table 2). One exception is the data set for the strong source 12, in which the data are divided into 89 bins of 91 s length. The probabilities given in column (10) of Table 2 are the probabilities that a random sample about the mean count rate per adopted time interval could yield a  $\chi^2$  value as large as the observed value. Only for probabilities much less than 0.01 should variability be seriously considered.

As can be seen in column (10) of Table 2, only for source 26 (SMC X-1), which is a previously recognized variable, is there any hint of variability. Other than SMC X-1, the only source

TABLE 1  
IPC OBSERVATIONS

SEQUENCE	R.A. (1950)	Decl. (1950)	EXPOSURE TIME (s)	PERIOD OF OBSERVATIONS <sup>a</sup>	
				Start	End
7988.....	00 <sup>h</sup> 53 <sup>m</sup> 15 <sup>s</sup>	-72°43'37"	16872	106 <sup>d</sup> 06 <sup>h</sup> 56 <sup>m</sup>	108 <sup>d</sup> 20 <sup>h</sup> 40 <sup>m</sup>
7988.....	01 08 00	-72 41 00	24150	105.02.45	106.18.28
7990.....	01 15 00	-73 30 00	12070	108.02.23	108.17.25
7991.....	01 27 00	-73 48 00	12255	107.01.57	107.17.50

<sup>a</sup> Start and end dates are given in day of year. All observations were made in 1980. Because of overhead time, the elapsed time between the start and end dates are longer than the total processed exposure time.

TABLE 2  
X-RAY SOURCE CANDIDATES IN THE SMC

Number (1)	R.A.(1950) (2)	Decl.(1950) (3)	Image (4)	HEAO 2 Flux (cts s <sup>-1</sup> ) (5)	Flux Error <sup>a</sup> (cts s <sup>-1</sup> ) (6)	Error Radius (7)	X-Ray Luminosity <sup>b</sup> (8)	R <sup>c</sup> (9)	Associated Probability (10)	Bins No./Lens (11)	Quality (12)
1A.....	00 <sup>h</sup> 45 <sup>m</sup> 56 <sup>s</sup>	-73°25'23"	7988	5.52(-3)	...	...	1.1	...	...	...	B
1B.....	00 45 30	-73 28 41	7988	1.06(-2)	2.5(-3)	39"	2	0.44	0.71	990/8	A
2.....	00 47 25	-73 30 29	7988	3.16(-3)	...	...	0.6	H	...	...	B
3.....	00 50 07	-72 48 14	7988	5.9(-3)	1.5(-3)	36	1.2	0.19	0.35	792/10	A
4.....	00 50 10	-73 27 45	7988	4.0(-3)	1.7(-3)	86	0.8	-0.73	0.73	880/9	B
5.....	00 50 37	-72 53 32	7988	1.9(-3)	...	...	0.4	S	...	...	B
6.....	00 51 08	-73 04 36	7988	6.4(-3)	1.4(-3)	36	1.3	0.62	0.29	565/14	A
7.....	00 51 39	-72 52 11	7988	1.4(-3)	...	...	0.3	S	...	...	C
8.....	00 52 13	-72 42 52	7988	8.8(-3)	2.8(-3)	35	1.8	0.76	0.49	880/9	A
9.....	00 53 13	-72 43 00	7988	7.6(-3)	2.5(-3)	37	1.5	0.40	0.49	880/9	A
10.....	00 53 15	-73 14 57	7988	4.2(-3)	1.2(-3)	60	0.8	...	0.11	880/9	D
11.....	01 01 27	-73 00 49	7989	4.2(-3)	...	...	0.8	...	...	...	B(?)
12.....	01 02 37	-72 17 56	7989	4.5(-1)	1.14(-2)	30	92.	-0.21	0.11	99/89	A
13.....	01 03 20	-72 38 46	7989	1.19(-2)	2.8(-3)	34	2.4	-0.10	0.96	630/14	A
14.....	01 03 55	-72 26 31	7989	1.8(-3)	...	...	0.4	H?	...	...	B
15.....	01 05 29	-72 40 25	7989	4.4(-3)	1.0(-3)	35	0.9	0.17	0.70	679/13	A
16.....	01 05 42	-72 51 12	7989	7.2(-3)	1.2(-3)	31	1.4	0.32	0.70	679/13	A
17.....	01 06 03	-72 59 21	7989	5.6(-3)	...	...	1.1	H	...	...	B
18A.....	01 07 04	-72 40 43	7989	3.5(-3)	9.0(-4)	36	0.7	0.45	0.20	589/15	A
18B.....	01 07 09	-72 43 51	7989	3.8(-3)	1.0(-4)	36	0.8	0.33	0.51	552/16	A
19.....	01 07 35	-72 52 47	7989	6.2(-3)	8.0(-4)	32	1.2	0.46	0.65	736/12	A
20.....	01 10 27	-72 47 03	7989	1.9(-3)	...	...	0.4	H?	...	...	C
21.....	01 10 23	-73 53 32	7990	8.0(-4)	2.1(-3)	52	0.2	-0.20	0.045	1249/4	D
22.....	01 12 43	-73 35 30	7990	2.4(-3)	1.3(-3)	...	0.5	0.46	0.35	833/6	D
23.....	01 14 32	-73 35 08	7990	2.2(-3)	...	...	0.4	...	...	...	D
24.....	01 15 09	-73 30 34	7990	3.0(-3)	...	...	0.6	H	...	...	C
25.....	01 15 10	-73 15 39	7990	6.4(-3)	1.5(-3)	...	1.3	1.00	0.31	833/6	B
26.....	01 15 48	-73 42 05	7990	6.0(-2)	3.7(-4)	31	12.	0.45	0.0089	294/17	A
27.....	01 16 12	-73 26 07	7990	3.7(-3)	1.5(-3)	59	0.7	-0.34	0.71	625/8	B(?)
28.....	01 17 20	-73 33 33	7990	2.4(-3)	...	...	0.5	H?	...	...	C
29.....	01 17 19	-73 41 12	7990	1.87(-2)	2.4(-3)	32	3.7	0.12	0.18	500/10	A
30.....	01 18 09	-73 16 49	7990	7.8(-3)	2.1(-3)	37	1.6	0.70	0.98	714/7	A
31.....	01 19 19	-73 37 12	7990	2.2(-3)	...	...	0.4	S?	...	...	C
32.....	01 19 40	-73 51 00	8991	2.5(-3)	...	...	0.5	...	...	...	C
33.....	01 25 32	-73 43 06	7991	1.5(-3)	...	...	0.3	S?	...	...	D
34.....	01 26 32	-73 36 31	7991	1.8(-3)	...	...	0.4	H?	...	...	D
35.....	01 27 16	-73 45 27	7991	6.3(-3)	1.4(-3)	...	1.2	0.08	0.83	644/8	A

<sup>a</sup> Quantities in parentheses indicate the associated exponents in powers of 10.

<sup>b</sup> Units of the X-ray luminosity are 10<sup>35</sup> ergs s<sup>-1</sup>.

<sup>c</sup> Hardness ratio is defined as  $R = (H - S)/(H + S)$ , where  $H$  represents the counts in the pulse-height-independent (PI) energy band corresponding to 0.8–3.5 keV, while  $S$  represents the counts in the PI energy band corresponding to 0.2–0.8 keV.

NOTES.—1A. A definite source and also seen by IKT. This source was flagged in the old software only. The source is easily seen in computer displays of low-energy channels. This plus the results of IKT suggest the source to be a SNR. This source is quite near to 1B, such that 1AB might be considered to be extended. However, 1B appears to have a hard spectrum. Both 1A and 1B are embedded or near the nebulosity, DEM 32. This nebula is very bright in H $\alpha$ .

1B. A definite source and also seen by IKT. The hard spectrum implies a stellar interpretation. Optical counterpart is suggested. (Also see comments for 1A.)

2. A definite source and also seen by IKT. Source was flagged on the old software, but not on the new. This source is near the edge of the field, possibly causing problems with the local detect algorithm of the new processing scheme.

3. A definite source and a new detection. Possible optical counterpart (see Table 3).

4. A definite source and also seen by IKT. The hardness ratio suggests that it is a SNR. This source was flagged by new software only.

6. A definite source and a new detection. Possible optical counterpart (see Table 3).

8. A definite source and also seen by IKT. This source has the hardest spectrum of any detected source. No optical counterpart is suggested, but it is assumed to be a stellar source.

9. A definite source and also seen by IKT. Possibly stellar, but no optical counterpart is suggested.

11. A likely new source. This source was flagged only with the old software. This source shows accurate structure in computer displays of the low-energy channels. This apparent source is seen in the extreme lower corner of I 7989 (Fig. 2). Because of the source's location we have given it a quality rating of B(?). If real, it is likely a SNR.

12. Previously identified as a SNR by Seward and Mitchell.

13. Previously identified as a SNR by Seward and Mitchell.

14. A definite source also seen by IKT. No optical counterpart is suggested but is assumed to be stellar.

15. A definite source and a new detection. The hardness ratio suggests a stellar source, but no optical counterpart is suggested. The source coincides with southernmost ridge of the emission of DEM 134.

16. A definite source and a new detection. The source appears to be hard, but no optical counterpart is suggested.

17. A definite source and a new detection. This source was only flagged on the old processing scheme. The source is easily seen I7989 (Fig. 2). The failure of the new software to flag this source is likely due to shadowing by the nearby supporting ribs.

18AB. A definite source and a new detection. This source appears to be extended or multiple stellar sources. Hardness ratios imply the latter interpretation. Possible optical counterparts are identified (see Table 3).

with a probability less than 0.1 is source 21. However, this candidate has an unusually low flux and a quality index of D and represents an unlikely detection.

Of course, the bin sizes of 10–16 minutes used in the  $\chi^2$  tests does not rule out the possibility of much shorter, possibly periodic variability on time scales of a few minutes or less. As well, we cannot rule out much longer time scale variability than the total time interval comprised by the time of the observation.

Sixteen sources have detections of the highest quality, A, as indicated in column (10). These sources were easily found both in the old and new processing schemes. In addition, they are easily seen in a visual examination of the computer display of the X-ray imagery sampling all of the X-ray energy channels. All of these sources have IPC count rates of  $3.8 \times 10^{-3}$  counts  $s^{-1}$  or greater ( $L_x \gtrsim 7 \times 10^{34}$  ergs  $s^{-1}$ ).

Nine additional sources have the second highest quality value, B (also see the notes to Table 2 for these sources). These sources were found in either the old or new processing scheme, but not both. However, these sources are clearly seen in the computer displays of the X-ray imagery. All sources with quality ratings of A or B, a total of 25 X-ray sources, can be confidently considered as definite detections.

We also find six X-ray sources which are indicated by a quality index C. These sources have been flagged either by the old or new processing scheme, but only appear to be possibly present in visual inspection of a computer display of the X-ray imagery sampling either the low, high, or total energy channels. These sources are considered as possible detections.

Finally, for the sake of completeness, we include a low-quality detection index, D. This category includes all software flagged detections, but which show no hint of an X-ray source in visual examination of the imagery. All sources in this category have IPC count rates  $\sim 2.4 \times 10^{-3}$  counts  $s^{-1}$ . We consider such candidates as unlikely detections.

To find counterparts to the X-ray sources at other wavelengths it is necessary to have reliable X-ray positions. Because of still yet to be understood systematic errors, the best IPC positions of X-ray sources are accurate to  $\sim 30''$  (Seward, private communication). These uncertainties make it difficult to find counterparts to the X-ray sources at other wavelengths, particularly in regions within the SMC where many candidate objects lie in the IPC fields. Identifying counterparts to the X-ray sources in Table 2 at other wavelengths will be the topic of section IV.

### III. THE INTRINSIC X-RAY LUMINOSITIES FOR SOURCES IN THE SMC

In general, the *Einstein* X-ray flux can be used to estimate the intrinsic X-ray luminosity of the source, providing the spectral nature of the source and the intervening interstellar absorption is known. Examination of 21 cm data of Hindmann (1967) for the SMC shows line-of-sight H I column densities of  $4\text{--}8 \times 10^{21}$   $\text{cm}^{-2}$  for the four IPC fields discussed here. Since

the SMC is near the south galactic pole, most of this observed gas is likely associated with the SMC. Furthermore, since the attenuation of X-rays in the energy range from 0.5 to 0.9 keV is determined primarily by oxygen K-shell absorption, and since the SMC is underabundant in oxygen by roughly a factor of 6–7 (Dufour, Shield, and Talbot 1982), then for purposes of determining X-ray attenuation, a gas column density of  $10^{21}$   $\text{cm}^{-2}$  with a solar composition is equivalent to  $6\text{--}7 \times 10^{21}$   $\text{cm}^{-2}$  for the SMC. These results indicate that there is little intervening X-ray attenuation for sources in the SMC. The low attenuation implies only small, typically less than a factor of 2, interstellar corrections in deriving intrinsic X-ray luminosities.

For X-ray sources which are SNRs in the SMC we assume that their emitted spectra are soft and typically represented by thermal bremsstrahlung and radiative recombination spectrum at  $10^7$  K (Raymond and Smith 1977). In this case, 1 IPC count  $s^{-1}$  corresponds to an intrinsic X-ray luminosity at the SMC of  $2.2 \times 10^{37}$  ergs  $s^{-1}$  in the *Einstein* 0.15–4.5 keV bandpass.

Conversely, if we consider an X-ray source with a power-law spectrum, as we might expect to find for sources analogous to galactic X-ray binaries, then 1 IPC count  $s^{-1}$  corresponds to an intrinsic X-ray luminosity in the SMC of  $3.1 \times 10^{37}$  ergs  $s^{-1}$ . This result is extremely insensitive to the spectral index of the power spectrum.

It is important to add that if the observed source possesses some intrinsic X-ray attenuation, in addition to that resulting from intervening interstellar material, then the intrinsic X-ray luminosity of the source producing the X-rays would be underestimated.

### IV. THE NATURE OF THE DETECTED SOURCES

#### a) Previously Detected X-Ray Sources

Four of the sources listed in Table 2 have been previously detected with shorter *Einstein* observing times by SM. These are source numbers 12, 13, 26, and 29. Only one source, 26 (SMC X-1), was detected previous to the work of SM. Another source, 29, was also previously identified by SM as HD 8191, a galactic foreground star. Our low count rate of  $6 \times 10^{-2}$  counts  $s^{-1}$  for SMC X-1 compared to 0.27 and 1.2 counts  $s^{-1}$  for the IPC and high resolution imager (HRI) observations of SM indicates that this source was much less active at X-ray energies during our observations. Our IPC count rate for HD 8191 was 0.0187 counts  $s^{-1}$  compared to the HRI derived flux of 0.008 counts  $s^{-1}$  given by SM. The other two sources in common to SM, 12 and 13, correspond to the sources (1E 0102.2–7219) and (1E 0103.3–7240), respectively, in their list. The work of SM identified No. 12 as a supernova remnant near N76, and No. 13 as a possible supernova remnant. Our deduced hardness ratios, like those of SM, indicate a soft X-ray spectra for both of these objects and further supports the SNR interpretation. None of the other sources listed by SM lie within the fields of view of the X-ray imagery presented here.

Since both sources, 12 and 13, are bright supernova rem-

#### NOTES TO TABLE 2—Continued

19. A definite source and a new detection (see Fig. 2).
25. A definite source and a new detection. This source was flagged only by the new software.
26. Previously identified as SMC X-1 = SK 160.
27. A definite source and a new detection. Although this source lies near the field center and was flagged by both old and new software, this source does not stand out in the computer displays of the imagery (also see text).
29. Previously identified as HD 8191 by Seward and Mitchell.
30. A definite source and a new detection. The source appears to be hard, but no optical counterpart is suggested.
35. A definite source and a new detection. Although the hardness ratio (0.08) could suggest a SNR, closer examination of the PHI bands shows the spectrum to have more similarities with SK 160 than the previously identified SNRs. No optical counterpart is suggested.

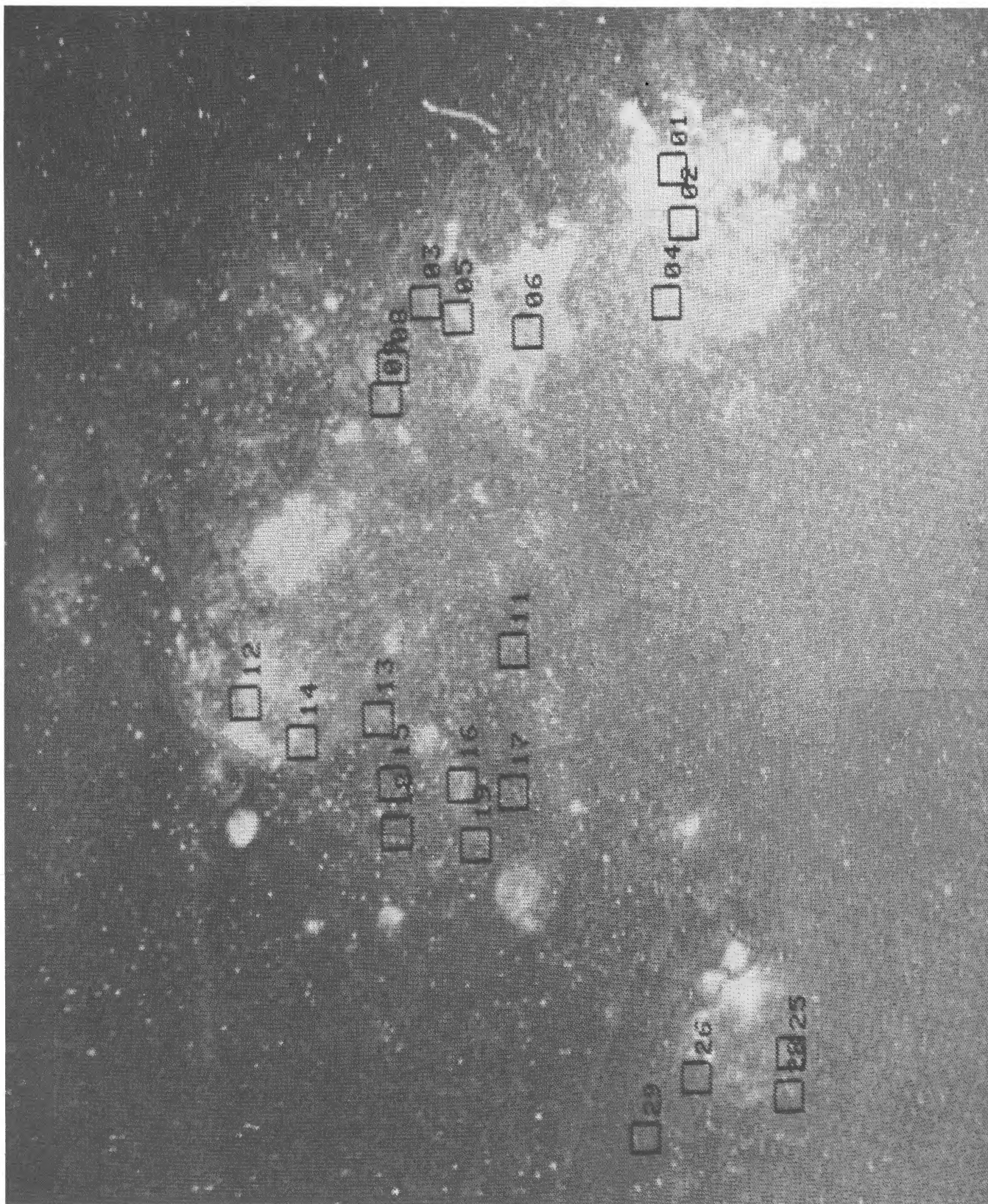


FIG. 1.—Approximate positions of X-ray sources in the SMC. The positions of the X-ray sources with definite detections (those with quality ratings of A or B as given in Table 2) are superposed upon narrow-band H $\alpha$  imagery of the SMC (Lasker 1979). One source (No. 34) lies at the extreme eastern portion of the wing of the SMC and is not shown.

nants at X-ray energies, one might expect the net X-ray source count rates from our results and those of SM to be quite similar. This is especially true, since both our data and that of SM were processed using a local detect algorithm (Seward, private communication) for determining the local background. However, our observations of source 12 gives  $0.457 \text{ counts s}^{-1}$ , while SM gives  $0.86 \text{ counts s}^{-1}$ . A similar discrepancy is found for No. 13, where our count rate of  $1.19 \times 10^{-2} \text{ counts s}^{-1}$  is again lower than that ( $7.6 \times 10^{-2} \text{ counts s}^{-1}$ ) of SM. These apparent discrepancies were explained when we examined the X-ray imagery for IPC field 7989. The source 12 was found to be at the edge of the field where vignetting is most extreme. In addition, part of the X-ray flux appears to have fallen outside the field of the detector. In the case of source 13, it was partially occulted by the support ribs of the IPC.

We have also compared our results with those of IKT. Even though the X-ray fields were selected to maximize the total spatial coverage of the SMC, there was still a significant overlap in fields chosen by IKT and our study. In Table 3, we present the detected sources which are in common to the fields of both studies. The source number as listed in Table 2, the IKT source number, position, and some indication of whether the spectrum of the source is hard (H) or soft (S) are listed. We cannot directly compare the hardness ratios between the two studies since the ratios were defined differently. However, they do show qualitative agreement. Also given in Table 3, is the error radius between the two studies as determined from the approximate difference between each source position of IKT and our study. In all, we find a total of 10 sources in common to both studies. Two of these sources, 12 and 13 (23 and 24 of IKT), were also detected by SM.

The sources in the overlap regions lie at the periphery of the fields and have a high likelihood of either being partially occulted by supporting ribs or being flagged only by the old data reduction software. Since the old software assumed that a uniform flat background, derived from the central region of the field, applied through each image, the fluxes deduced in this manner are likely underestimates. Only fluxes from sources not occulted by the supporting ribs and flagged with the new data reduction software, can be compared. The local detect algorithm in this software provides fairly reliable X-ray fluxes, and

comparisons of the derived fluxes for the sources 1B, 8, and 9 in Table 3 show relatively good agreement.

#### b) New X-Ray SNRs?

The spatial resolution of the IPC is quite low and generally cannot be used to distinguish between SNRs and stellar point sources at distances of the SMC. However, the X-ray spectra of SNRs are quite soft and can be used to separate out SNRs from harder, likely stellar sources. The IPC spectral resolution ( $E/dE$ ) is also quite low, being on the order of 1–2, but it can provide some rough indication of the softness or hardness of the X-ray spectra. Unfortunately, the hardness ratio ( $R$ ) given here cannot be directly compared with SM or Long *et al.* Two of the softest sources given in Table 2 (Nos. 12 and 13) have previously been identified as SNRs (Seward and Mitchell 1981; Mills *et al.* 1982; Mathewson *et al.* 1983). The hardness ratios of two other sources (4 and 27) indicate soft spectra. A further detailed examination of the invariant pulse height spectral information, gives additional evidence for a soft X-ray spectrum for source 4 and further supports the SNR interpretation. However, a similar detailed examination of the pulse height data indicates that source 27 may not be as soft as the hardness ratio in Table 2 suggests. (Also see footnotes to Table 2). Another source, No. 11, as seen in Figure 2 at the extreme corner of image I7989, shows a diffuse structure suggestive of a SNR. Thus, these results indicate the detection of two, possibly three, new X-ray SNRs in the SMC.

One might also consider sources 18A and 18B as a single extended source and a SNR. However, their spectra seem to be hard and uncharacteristic of SNRs. In such cases, the implied extended nature can best be explained by multiple unresolved stellar sources rather than SNRs.

Radio, and optical observations of SNRs and SNR candidates in the Magellanic clouds and how they compare with X-ray observations have been discussed by Mathewson *et al.* (1983) and Mills *et al.* (1982). These studies identify a total of six supernova remnants in the SMC, where four of these have been seen previously with *Einstein* by SM. Neither of the two other SNRs seen at radio and optical wavelengths lie within the fields of the IPC imagery discussed here.

We have also compared the positions of sources 4, 11, and 27

TABLE 3  
X-RAY SOURCES IN OVERLAY REGIONS OF THE SURVEYS OF IKT AND THIS STUDY

SOURCE NUMBER (Table 2)	IKT RESULTS					
	Number	R.A.	Decl.	Flux ( $\times 10^{-3} \text{ ct s}^{-1}$ )	Spectrum	ERROR RADIUS
1A .....	2	00 <sup>h</sup> 45 <sup>m</sup> 34 <sup>s</sup>	−73°25′21″	5.8	S	99
1B .....	1	00 45 32	−73 28 51	2.4 <sup>a</sup>	H	13
	3	00 46 05	−73 21 21	0.6	?	...
2 .....	5	00 47 15	−73 30 15	0.6	?	47
4 .....	7	00 49 54	−73 26 48	4.6	S	92
8 .....	10	00 52 17	−73 42 46	2.4 <sup>a</sup>	H?	19
9 .....	11	00 53 20	−73 42 46	1.2 <sup>a</sup>	H	56
12 .....	22	01 02 25	−73 18 00	157	S	54
13 .....	23	01 03 23	−72 39 20	16.8	S	37
14 .....	24	01 03 45	−72 28 30	2.8	H?	127

<sup>a</sup> Fluxes from these IKT sources are the only ones that can be compared with counterparts in Table 2. Other sources from Table 2 listed here were either partially occulted by supporting ribs, or the fluxes given in Table 2 are derived from old data reduction of the X-ray images. Fluxes in Table 2 are probably underestimations of the actual X-ray fluxes in these cases.



TABLE 4  
POSSIBLE OPTICAL STELLAR COUNTERPARTS

X-Ray Source	AV Number	Spectral Type <sup>a</sup>	$-M_{\text{bol}}$	Errors Displacement	Comment
1AB .....	26	O7+nebula	10.4	63"	Sk 18; also see comments to Table 1
3 .....	111	B1:	7.1	15	
6 .....	138	B0:	7.7	3	
18AB .....	462	B1 Ia-B0 I:	9.0	90	18AB appears to be an extended or multiple source
26 <sup>b</sup> .....	490	B0 Iwp	8.3	18	SMC X-1 = Sk 160
29 <sup>b</sup> .....	HD 8191				Foreground object

<sup>a</sup> Accurate spectral types are from Humphreys 1983, and references cited therein. The uncertain or less reliable classifications are from the AV list.

<sup>b</sup> Previously identified sources and optical counterparts. Previous HRI data suggest the optical counterparts are definite (see text).

with the  $H\alpha + [N II]$  emission survey of Davies, Elliot, and Meaburn (1976), and the  $H I$ ,  $[O III]$ , and  $[S II]$  data of one of the authors (T. R. G.). We found no coincidences with positions of shell nebulae and possible SNR in the SMC as given by Davies, Elliot, and Meaburn. Source 4, best coincided with the numbered  $H II$  regions DEM 65 and DEM 66 in the  $H II$  region list of Davies *et al.* (1976). However, both of these nebulosities are described as diffuse. No coincidences with  $H II$  regions listed by Davies *et al.* are found for the X-ray sources 11 and 27. The closest  $H II$  region in the list of Davies *et al.*, DEM 159, lies some 3' to the west of source 27.

It is interesting to note that even though the exposure times of the IPC images discussed here are much longer than that of SM, few additional X-ray SNRs (possibly two or three) are seen. This suggests that the sample of X-ray emitting SNRs is reasonably complete for the four fields discussed here.

### c) Stellar Sources

Presumably, most, if not all, of the identified sources in Table 2 with hardness ratios larger than the suspected SNRs mentioned above are due to X-ray emission from stellar systems. Two of these sources have been previously identified as being associated with stars. Specifically, source 26 is SMC X-1 (Sanduleak 160) and source 29 has been identified with a foreground star (HD 8191) in our own Galaxy. Both of these objects were observed by the HRI aboard *Einstein*, and there is no doubt about the identification of the optical counterparts. We have further searched for positional coincidences between the hard sources in Table 2 and O and B stars in the SMC, as listed by Azzopardi and Vigneau (1982). We have found close coincidences for four hard sources. These coincidences are given in Table 4. In each column of Table 4 the X-ray source number is given, followed by the Azzopardi and Vigneau (AV) number of the OB star optical candidates, approximate stellar spectral type, bolometric magnitude, and error "displacement" in arc seconds. The colons following the spectral types and bolometric magnitudes denote significant uncertainties principally as a result of the approximate spectral type provided by objective-prism spectroscopy in the AV list. The error circles only reflect the differences between the stated stellar positions from Azzopardi and Vigneau and the X-ray positions from Table 2 and do not take into account any additional positional uncertainties. We have listed all O and B stars given by Azzopardi and Vigneau within 90" of the X-ray positions. The positional coincidences seem quite good, especially

in the case of X-ray source 6 and the O star AV 138. However, simply given the 30" optimum positional uncertainties of the IPC, we must await future X-ray experiments with spatial resolutions comparable to the HRI aboard *Einstein* to confirm these identifications. (Also see the more extended discussion in § V.)

Except for HD 8191, which had been previously identified by SM, we have found no coincidences with galactic stars in the SAO catalog for any of the hard sources. This is not to say that some of the sources in Table 2 are not foreground galactic stars. Indeed, the *Einstein* stellar X-ray survey of Vaiana *et al.* (1981) shows that stars in general, regardless of spectral type and luminosity, may be significant X-ray emitters. However, since the detected X-ray sources are concentrated in the body of the cloud (except source 35, found in IPC field number 7991, which lies at the extreme eastern position of the wing of the SMC), it is unlikely that more than a few of the sources are either foreground galactic stellar sources or background extragalactic sources not associated with the SMC.

## V. THE NATURE OF THE SMC HARD SOURCES

### a) X-Ray Binaries

In our own Galaxy, the X-ray binaries have typical X-ray luminosities of  $L_x > 10^{35}$  ergs  $s^{-1}$ . By contrast, the SMC hard X-ray sources in Table 2 have X-ray luminosities,  $34.0 \leq \log L_x \leq 35$ , definitely below those of galactic X-ray binaries. The only galactic analogs appear to be the X-ray Be stars, which characteristically exhibit X-ray luminosities in the range  $33 \leq \log L_x \leq 35$ . These Be stars are suspected to be binaries and to have neutron star companions (Rappaport and van der Heuvel 1982). Of these,  $\gamma$  Cas (B0.5 V) and X Per (O9.5 III-V) appear to be prototypes. Their X-ray properties have been discussed in White *et al.* (1982). Evidence strongly supports the interpretation that the X-ray emission in these galactic objects is due to accretion onto a neutron star. The X-ray luminosities derived for the hard sources in Table 2 are similar to the X-ray Be stars. Yet, unlike the galactic X-ray Be stars, which show X-ray variability on the order of 10 minutes, none of the SMC sources show any evidence of variability in the temporal analysis of the IPC data. Variability at these time scales should be detectable in the *Einstein* data. It is tempting to suggest that the sources listed in Table 3 are X-ray Be stars, but the lack of established variability is disturbing.

Another possible interpretation is that the hard SMC

sources are analogs to the cataclysmic variables in our own Galaxy. These galactic objects are interacting binary systems and are thought to contain accreting white dwarfs. Yet the inferred peak X-ray luminosities for galactic cataclysmic variables, as seen during visual outburst, are below  $10^{34}$  ergs  $s^{-1}$  (see the review by Cordova and Mason 1983). This seems too low compared to the X-ray luminosities for the SMC hard sources.

The cataclysmic variables show a wide range of time scales for X-ray variability. Periodic variability is often seen on time scales of tens of seconds, but sometimes as long as tens of minutes (Cordova and Mason 1983). Usually X-ray emission is detected only during optical outbursts. The rise in emission at visual wavelengths during an outburst typically occurs in less than 1 day, while the decline takes place, more slowly, over a period of a few days. A rise of at least a factor of 100 in X-ray emission during optical outbursts is implied, as in the case of U Gem (Mason *et al.* 1978).

Although the results of the variability analysis (cols. [10] and [11] of Table 2) show no evidence of variability, perhaps the strongest evidence against variability like that expected from cataclysmic variables comes from Table 3. Specifically, for every hard source identified by us in the overlap region between the two surveys, a counterpart can be found in the results of IKT. If the sources were unusually luminous cataclysmic variables, it would argue that all of these sources were in outburst during both sets of observations. Since the IKT results in Table 3 are from IPC image 3926, which was acquired many months prior to our data, the cataclysmic variable interpretation seems very unlikely.

#### b) Normal O and B Stars?

Observations with the *Einstein Observatory* have shown normal galactic O and B stars to be emitters of X-rays (White and Long 1981; Cassinelli *et al.* 1981; Seward *et al.* 1979). Yet the X-ray luminosity of these objects is in the range  $31 \lesssim \log L_x \lesssim 33$ , much below those deduced for the hard SMC sources. Even lower X-ray luminosities are found for other galactic stars of later spectral type (Vaiana *et al.* 1981). Despite this, as we will discuss below, it still may be premature to rule out normal O and B stars as the sources of the X-ray emission in the SMC.

One theoretical picture indicates that the observed X-ray emission in normal O and B stars originates from hot ( $T \approx 10^{6-7}$  K) stellar coronae. The intrinsic X-ray emission from these coronal regions should be quite large. However, this emission is extensively blanketed by much cooler X-ray attenuating stellar winds overlaying the stellar coronae (see Hearn 1975; Cassinelli *et al.* 1981; Waldron 1984). The results of Waldron suggest that the attenuation of the overlying wind can be quite substantial. For example, he finds that the X-ray luminosity of a typical base corona is  $10^3$ – $10^4$  times that of the final emergent luminosity seen beyond the stellar wind.

Alternate models which suggest that the X-ray emission occurs further in the wind, possibly even at large distances from the star, due to the shocks arising from radiative instabilities have been proposed (Lucy 1982). However, the coronal base models best reproduce the overall shape and X-ray luminosity of O and B stars seen with the IPC aboard *Einstein*, although there still is some question about the strengths of the K-shell absorption edges. The coronal base models predict more pronounced edges in comparison to models which have

shocks embedded in the stellar wind (Lucy 1982; Waldron 1984).

The results of Waldron suggest that elemental abundance differences might have pronounced effects on the final emergent X-ray luminosities in the coronal base models. Waldron (1984) finds that as long as the cooling is rapid, the thickness of the effective coronal region remains small. However, as is seen in Shapiro and Moore, (1976), cooling at coronal temperatures arises from metals. The primary coolants at  $\log T > 6.0$  are Fe, Mg, Si, and S, at  $5.5 < \log T < 6.0$  it is Ne, and at cooler temperatures (i.e.,  $4.8 < \log T < 5.5$ ) the elements C, O, and He becomes strong coolants. The lower metal abundances in the SMC imply less effective cooling and perhaps thicker base coronal regions for O and B stars of the SMC than for similar stars of the Milky Way. In addition, as is seen in Figure 5 of Waldron, any acceptable theoretical fit to the observed X-ray spectra for galactic O and B stars implies that the final observable emergent X-ray luminosity ( $L_x^0$ ) would increase dramatically for any slight increase in the total intrinsic X-ray emission measure (EM)  $L_x$  of the corona. Such an effect would naturally lead to significantly larger X-ray luminosities for normal O and B stars in the SMC where metals are deficient (Dufour, Shields, and Talbot 1982; Bruhweiler, Parsons, and Wray 1982). One might also see a similar effect for stars in the LMC as well, but the elemental abundances in the LMC reflect more closely those of the Milky Way, and such effects would be much less pronounced. Recently, Waldron (private communication) has performed detailed calculations, in which an elemental mix consistent with the SMC (Dufour *et al.*) was used. For a star similar to the supergiant  $\epsilon$  Ori (B0 Ia) the X-ray luminosity ( $L_x^0$ ) was increased by a factor of 40 over that predicted using a solar composition. Thus, there is quantitative theoretical evidence that "normal" O and B stars might well explain the presence of sources with  $10^{34} \lesssim L_x^0 \lesssim 10^{35}$  in the SMC. If this picture is correct, it would require that the ratio of the  $L_x^0$  to the total stellar bolometric luminosity  $L_x^0/L_{\text{bol}}$  is  $\sim 10^{-5}$  rather than  $10^{-7}$  as seen for O and B stars in our Galaxy.

If OB stars in the SMC possess X-ray luminosities a factor of 40 greater than corresponding objects with similar bolometric magnitudes in the Galaxy, then a detection threshold of  $L_x^0 = 10^{34}$  ergs  $s^{-1}$  for the SMC corresponds to OB stars of  $-M_{\text{bol}} = 9.8$ . Indeed, only the most luminous stars in the SMC and in the list of AV should be detected in our data.

Unfortunately, most of the stars in the AV list have spectral types determined using very low resolution spectral data and cannot be used to derive reliable bolometric magnitudes. However, fairly accurate spectral types for  $\sim 70$  stars in the SMC are available (Humphreys 1983; Garmany and Conti 1985; Walborn 1983).

Of these stars, six OB stars indicate  $-M_{\text{bol}} > 9.8$ . These stars are Sanduleak objects 18, 78, 80, 101N, 108, and 157. Four of these objects lie within  $60''$  of the X-ray source positions given in Table 2 (also see Table 3) or in Table 1 of IKT, while no coincidences are found for Sk 101N and 108 in the source list of IKT. The star, Sk 18 (see Table 4), lies close to the positions of the sources 1A and 1B. These sources are discussed in the notes of Table 2. This star, as well as the X-ray sources 1A and B, seem associated with the nebulosity DEM 31. This nebulosity is very prominent in  $H\alpha$  and is easily visible in the photographic data of Davies, Elliot, and Meaburn (1976). In the case of the second source, which is in the IKT and SM data, but not that data presented here, it corresponds to the posi-

tions of the two stars, Sk 78 and 80, and the nebulosity, NGC 346. This nebula and its association with an X-ray source has been previously discussed by SM, IKT, and Walborn and Blades (1986). The nebula, NGC 346, is the largest H II region in the SMC, and Walborn and Blades have shown that there are several previously unrecognized very early O stars embedded in this nebulosity. The diffuse X-ray emission from both NGC 346 and DEM 31 may be the result of the stellar wind cavities similar to that of the Carina Nebula (Seward *et al.* 1979; Weaver *et al.* 1977; Bruhweiler *et al.* 1980). Finally, the star Sk 157 is identified with the questionable source 23, which is given only a quality index of D in Table 2.

If the most luminous stars are responsible for the observed X-ray emission discussed above, it is still unresolved whether the bulk of this emission arises in a base coronal region, just above the photosphere of single or multiple stars, or if it principally originates by soft, diffuse emission in the cavities carved out by the stellar winds of these stars.

There are 17 SMC sources in Table 2 with quality ratings of A or B and with hard X-ray spectra which previous to this study had no optical identified counterparts. (We have counted 1AB and 18AB as single sources and also included 35 in this total.) Of these, six (6, 8, 9, 17, 25, and 30) do not appear to lie within 60" of the boundaries of H $\alpha$  emission as delineated in the figures presented in Davies, Elliot, and Meaburn. If young objects tend to be associated with nebulosity, and considering that H $\alpha$  emission covers a significant fraction of the plane of the sky toward the SMC, this correlation only slightly favors a young stellar population being responsible for the observed X-ray sources.

An important point, as shown in Table 4, is that we find five AV stars within 90" of our X-ray positions. If we take this as a measure of the density of the AV stars in the region, we might expect  $(5 \pm [5]^{1/2}) * (20/90)^2 = 0.25 \pm 0.11$  stars within 20". We actually find three. If the mean density is  $0.25 + 0.11$ , or 0.36 stars per 20" circle, then the chances of finding three or more is 0.014, which is quite small. Therefore, the three positional coincidences within 20" given in Table 4 are significant and suggest that at least some of the X-ray sources represent a young stellar population.

It is interesting that Walborn and Blades suggest that many of the most luminous OB stars in the SMC have yet to be identified. Certainly, the paucity of identified stars at the highest luminosities as noted by Humphreys does not contradict this interpretation. Whether further spectroscopic studies will show additional coincidences between the most luminous SMC OB stars and the hard X-ray sources in Table 2 remains to be seen.

Two of us (F. C. B. and D. A. K.) are currently analyzing ground-based spectrophotometry of many bright stars near the X-ray source positions given in Table 2. Even though many previously unknown luminous early-type stars have been identified, the results are still inconclusive and must await more detailed analysis.

## VII. CONCLUSIONS

We have presented our results for deep IPC imagery covering ~50% of the main body and wing of the Small Magellanic Cloud. These results show the presence of 25 X-ray sources. Of the 12 newly identified sources, two, possibly three, appear to be supernovae remnants. The other identified sources appear to have hard spectra and are presumably associated with stars. The hard sources (Table 2) are unusual in that their 0.15–4.5 keV *Einstein* X-ray luminosities fall in the range  $34 \lesssim \log L_x \lesssim 35$ . This range is much lower than that found for typical galactic X-ray binaries and a factor of 100 larger than the X-ray emission found for normal luminous O and B stars of our own Galaxy. If elemental abundance differences between our Galaxy and the SMC played only a secondary role in determining the X-ray characteristics of sources, then the hard SMC sources bear the closest resemblance to the galactic X-ray Be stars. However, the lack of apparent variability in the SMC sources is strikingly at variance with the variability observed for all X-ray emitting Be stars in the Milky Way. On the other hand, if the chemical composition is of importance, as preliminary calculations suggest, these sources might be normal luminous O and B stars in the SMC. However, since there may still be many, yet to be identified, luminous OB stars in the SMC, this frustrates attempts at finding luminous optical counterparts. Also, the lack of strong correlation between hard X-ray sources and H $\alpha$  emission does not particularly favor OB stars as an explanation for the SMC hard sources. Thus, one must consider that the nature of the hard X-ray sources remains unknown.

The authors wish to acknowledge the assistance of the staff associated with the *Einstein X-Ray Observatory*, especially that of Fred Seward. One of us (F. C. B.) wishes to thank Wayne Waldron and Joseph Cassinelli for discussions on the possible effects of metallicity upon stellar X-ray emission. We further acknowledge an anonymous referee for valuable comments and the use of the Interactive Astronomical Data Analysis Facility at Goddard Space Flight Center. We also thank Barry Lasker for allowing us to use of his narrow bandpass imagery of the SMC.

## REFERENCES

- Azzopardi, M., and Vigneau, J. 1982, *Astr. Ap. Suppl.*, **50**, 291.  
 Bruhweiler, F. C., Gull, T. R., Katatos, M., and Soňa, S. 1980, *Ap. J. (Letters)*, **238**, L27.  
 Bruhweiler, F. C., Parsons, S. B., and Wray, J. D. 1982, *Ap. J. (Letters)*, **256**, L49.  
 Cassinelli, J. P., Waldron, W. L., Sanders, W. T., Harnden, F. R., Rosner, R., and Vaiana, G. S. 1981, *Ap. J.*, **250**, 677.  
 Clark, G., Doxey, R., Li, F., Jernigen, J. G., and van Paradijs, J. 1978, *Ap. J. (Letters)*, **221**, L37.  
 Cordova, F. A., and Mason, K. O. 1983, in *Accretion Driven Stellar X-Ray Sources*, ed. W. H. G. Lewin and E. P. H. J. van den Heuvel (Cambridge: Cambridge University Press), p. 147.  
 Davies, R. D., Elliot, K. H., and Meaburn, J. 1976, *Mem. R.A.S.*, **81**, 89.  
 Dufour, R. J., Shields, G. A., and Talbot, R. J. 1982, *Ap. J.*, **252**, 461.  
 Forman, W., Jones, C., Cominsky, L., Julien, P., Murray, S., Peters, G., Tananbaum, H., and Giacconi, R. 1978, *Ap. J. Suppl.*, **38**, 357.  
 Garmany, C. D., and Conti, P. S. 1985, *Ap. J.*, **293**, 407.  
 Giacconi, R., *et al.* 1979, *Ap. J.*, **230**, 540.  
 Harnden, F. R., Fabricant, D. G., Harris, D. E., and Schwarz, J. 1984, *Smithsonian Ap. Obs. Spec. Rept.*, No. 393.  
 Hearn, A. G. 1972, *Astr. Ap.*, **19**, 417.  
 ———, 1975, *Astr. Ap.*, **40**, 277.  
 Hindman, J. V. 1967, *Australian J. Phys.*, **20**, 147.  
 Humphreys, R. M. 1983, *Ap. J.*, **265**, 176.  
 Inoue, H., Koyama, K., and Tanaka, Y. 1983, in *IAU Symposium 101, Supernova Remnants and Their X-Ray Emission*, ed. J. Danziger and P. Gorenstein (Dordrecht: Reidel), p. 535.  
 Lasker, B. 1979, *Publ. A.S.P.*, **91**, 153.

- Leung, C., Kellogg, E., Gursky, H., and Tananbaum, H. 1971, *Ap. J. (Letters)*, **170**, L67.
- Long, K. S., Helfand, D. J., and Grabelsky, D. A. 1981, *Ap. J.*, **248**, 925.
- Long, K. S., and White, R. L. 1980, *Ap. J. (Letters)*, **239**, L65.
- Lucy, L. B. 1982, *Ap. J.*, **255**, 286.
- Mason, K. O., Lampton, M., Charles, P., and Bowyer, S. 1978, *Ap. J. (Letters)*, **226**, L129.
- Mathewson, D. S., Ford, V. L., Dopita, M. A., Touhy, I. R., Mills, B. Y., and Turtle, A. J. 1984, *Ap. J. Suppl.*, **55**, 189.
- Mills, B. Y., Little, A. G., Durdin, J. M., and Kesteven, M. J. 1982, *M.N.R.A.S.*, **200**, 1007.
- Osmer, P. S. 1973, *Ap. J.*, **181**, 327.
- Price, R., Groves, D., Rodrigues, R., Seward, F., Swift, C., and Toor, A. 1971, *Ap. J. (Letters)*, **168**, L7.
- Przybylski, A. 1972, *M.N.R.A.S.*, **159**, 155.
- Rappaport, S., and van den Heuvel, E. P. J. 1982, in *IAU Symposium 98, Be Stars*, ed. M. Jасhek and H. G. Groth (Dordrecht: Reidel), p. 327.
- Raymond, J. C., and Smith, B. W. 1977, *Ap. J. Suppl.*, **35**, 419.
- Seward, F. D., Forman, W. R., Giacconi, R., Griffith, R. E., Handen, F. R., Jones, C., and Pye, J. P. 1979, *Ap. J. (Letters)*, **234**, L55.
- Seward, F. D., and Mitchell, M. 1981, *Ap. J.*, **243**, 736.
- Shapiro, P. R., and Moore, R. T. 1977, *Ap. J.*, **207**, 460.
- Walborn, N. R. 1983, *Ap. J.*, **265**, 716.
- Walborn, N. R., and Blades, J. C. 1986, *Ap. J. (Letters)*, **304**, L17.
- Waldron, W. L. 1984, *Ap. J.*, **282**, 256.
- Weaver, R., McCray, R., and Caster, J. 1977, *Ap. J.*, **218**, 377.
- White, N. E., Swank, J. H., Holt, S. S., and Parmar, A. N. 1982, *Ap. J.*, **263**, 277.
- Vaiana, G. S., et al. 1981, *Ap. J.*, **245**, 163.

FREDERICK C. BRUHWEILER: Department of Physics, Catholic University of America, Washington, DC 20064

THEODORE R. GULL: Code 683, NASA Goddard Space Flight Center, Greenbelt, MD 20771

DANIEL A. KLINGLESMTIH III: Code 684, NASA Goddard Space Flight Center, Greenbelt, MD 20771

SABATINO SOFIA: Department of Astronomy, Yale University, New Haven, CT 06511